Global Ecology and Conservation 58 (2025) e03441

Contents lists available at ScienceDirect

Global Ecology and Conservation

journal homepage: www.elsevier.com/locate/gecco

The precipitous decline of a gray fox population

Max R. Larreur [a,*], Clayton K. Nielsen [a], Damon B. Lesmeister [b], Guillaume Bastille-Rousseau [a]

[a] Cooperative Wildlife Research Laboratory, Southern Illinois University, 1263 Lincoln Dr, Carbondale, IL 62901, USA
[b] USDA Forest Service, Pacific Northwest Research Station, 3200 SW Jefferson Way, Corvallis, OR 97331, USA

ARTICLE INFO

Keywords:
Urocyon cinereoargenteus
Occupancy
Spatial model
Carnivore
Population decline

ABSTRACT

Gray fox (*Urocyon cinereoargenteus*) populations have apparently declined across the Midwestern United States which may be reflected in their distributional patterns and occupancy. To assess the severity of gray fox population declines and potential changing space use patterns, we used two temporally independent datasets collected using camera traps at the same sites during 2008–2010 and 2022–2023 within a 16,058-km^2 area of southern Illinois, USA. We then developed three predictive occupancy models that allowed comparison of gray fox spatial patterns and occupancy estimates over time. We assessed pairwise model predictive occupancy estimates using relative rank correlation and density plot overlap. Naïve occupancy (i.e., $n_{detected}/n_{surveyed}$) of gray fox declined from 0.20 to 0.06 between our two time periods. Predicted occupancy ranged from 0.01–0.47 to 0.11–0.43 between past and future spatial models, respectively, indicating stable gray fox occupancy and space use patterns. The contemporary model had predicted occupancy ranging from 0.02 to 0.10, a 4-fold decline in occupancy estimates across 99 % of our study extent. Most habitat features had different directional effects on gray fox occupancy between our two temporal periods, illustrating the complexity of gray fox habitat preferences and a shift in their ecology. Our study highlights the need for increased conservation and management of gray fox populations as their populations have indicated evident declines across the Midwest.

1. Introduction

Carnivores across the globe are facing unprecedented population declines and occupy smaller portions of their historic distributional ranges due to habitat loss and fragmentation, prey population declines, disease, rodenticides, and interspecific competition (Gese, 2001; Gabriel et al., 2012; Ripple et al., 2014; Meyer et al., 2015; Uzqueda et al., 2020; Marneweck et al., 2021). Increasing anthropogenic influences can exacerbate these destructive habitat changes, influencing how carnivores are distributed across the landscape (Cooper et al., 2012; Meyer et al., 2015; Creel et al., 2018; Manlick and Pauli, 2020; Davis et al., 2021). Removal of carnivores, and for some species their potential role as apex predators, can exacerbate effects caused from mesopredator release which potentially suppress populations of competing smaller-bodied predators and prey species (Prugh et al., 2009; Bergstrom, 2017). To develop proper management practices for these smaller-bodied predators, it is essential to understand natural and anthropogenic influences on their distributions and how these changes over time. This can be accomplished through repeated sampling and the comparison of new and previously developed spatial models using independent data, to ensure updated and accurate insights into

* Corresponding author.
E-mail address: maximillian.larreur@siu.edu (M.R. Larreur).

https://doi.org/10.1016/j.gecco.2025.e03441
Received 13 November 2024; Received in revised form 14 January 2025; Accepted 16 January 2025
Available online 21 January 2025

mesopredator distributions and demography (Woolf et al., 2002; Rich et al., 2017).

Spatial models are fundamental tools in ecology, helping explain how environmental factors and processes influence mesopredator space use and demographics (Nielsen and Woolf, 2002; LaRue and Nielsen, 2011; Guillera-Arroita et al., 2015; Lesmeister et al., 2015; Amspacher et al., 2021). Over the past few decades, spatial modeling has become essential for conservation, enabling biologists to assess predictive accuracy across broad temporal and spatial scales (Magness et al., 2010). This advancement allows for repeated sampling and the comparison of models built over significant periods, ensuring robust data and accurate predictions of species distribution (Austin, 2002; Elith and Burgman, 2003; Hernandez et al., 2006; Kwon et al., 2016). Continual reassessment of mesopredator responses to landscape factors is crucial for effective conservation and adaptive management plans (Elith et al., 2006; Gormley et al., 2011; Perkins-Taylor and Frey, 2020). Developing spatial models representing past, expected, or contemporary distributions allows for straightforward comparisons and hypothesis testing that can assist in identifying emerging threats or changes in habitat use that should be addressed. Differences between spatial models may reflect shifts caused by competitive interactions, population declines, or landscape changes, offering deeper insights into dynamic influences on species space use (Street et al., 2017). Additionally, similarity statistics (Warren et al., 2008; Donaldson et al., 2014; Hedrick et al., 2023) from these comparisons can highlight the degree of consistency or divergence in habitat associations over time, further informing conservation strategies.

Using data evaluation methods to compare the consistency of predictive estimates between independent datasets can bolster conservation decisions for mesopredators such as gray foxes (*Urocyon cinereoargentus*), whose populations have evidently declined across the Midwestern United States (Elith and Graham, 2009; Cooper et al., 2012; Guillera-Arroita et al., 2015; Lesmeister et al., 2015; Bauder et al., 2020). Gray foxes, one of the largest fox species in North America (3 – 7 kg), are an understudied mesopredator with limited knowledge on their distribution and population status (Cooper, 2008; Cooper et al., 2012; Lesmeister et al., 2015; Allen et al., 2021). Considered a predominantly woodland mesopredator, selecting for areas with ample tree cover and dense understory, gray fox distribution ranges from southern Canada into northern South America (Gittleman, 1985; Cypher, 2003). Annual harvests in Illinois during 1976–1989 were 3200 individuals and had declined to < 40 by 2015 (Bauder et al., 2020; Williams et al., 2020). Furthermore, Lesmeister et al. (2015) found that gray fox in southern Illinois had higher extinction rates than colonization rates which can indicate a declining population. Currently, gray fox are designated as a 'watch list' species with the Illinois Department of Natural Resources (hereafter, IDNR), indicating that this species has poorly known distributions, trends, and habitat needs (IDNR, 2005).

Using camera trap data in an occupancy modeling framework (MacKenzie et al., 2017), we developed 3 spatial models for gray fox in southern Illinois to assess potential changes in overall occupancy and spatial patterns in occupancy and potential drivers of those changes. Model 1 used data collected during 2008–2011 to represent past predictions of gray fox occupancy. Model 2 projects habitat relationships measured in Model 1 by extrapolating it using updated spatial layers reflecting current landscape conditions. Model 3 represents predictions of gray fox space use during 2022–2023. We also generated four different scenarios explaining changes in gray fox occupancy across the landscape (Table 1). These scenarios explain the how changes in occupancy (e.g., increase, decrease, or no change) of gray fox would influence the spatial pattern of occupancy assessed by relative rank correlation and density plots. We hypothesized an overall decline in occupancy (Lesmeister et al., 2015), but that spatial patterns would remain consistent between the two sampling periods based on relative rank correlation (Scenario B, Table 1). Furthermore, we predicted that Models 1 and 2 would show relatively unchanged occupancy estimates across our study extent, suggesting that the changes in gray fox occupancy are not attributable to change in landscape characteristics.

2. Methods

2.1. Study area

We conducted research in the 16 southernmost counties in Illinois (Fig. 1), which contain a human density of 19.7 persons/km^2 (United States Census Bureau, 2023). This area consists of 16,058 km^2 of private and public land and > 24 state and federally managed lands including the Shawnee National Forest (1075 km^2), Crab Orchard National Wildlife Refuge (178 km^2), and Cypress Creek National Wildlife Refuge (61 km^2). During January–April 2008–2010 the mean temperature in the study area was 6.28 $\pm$ 8.45 °C (range: −21.31 to 28.49 °C) with a mean precipitation of 0.18 $\pm$ 0.52 cm. During January–April 2022–2023 mean temperature was 7.69 $\pm$ 7.39 °C (range: −16.88 to 28.35 °C) with a mean precipitation of 0.24 $\pm$ 0.75 cm (range: 0–9.15 cm; Muñoz Sabater, 2019).

Our study area consisted of a mosaic landscape largely covered by agricultural lands (52 %), primarily comprised of corn (*Zea*

Table 1
Four scenarios and associated predictions regarding potential changes in gray fox occupancy. Two aspects of gray fox occupancy are distinguished, overall occupancy and spatial patterns of occupancy. Density plots compared overall occupancy across different spatial models and highlight potential decline in overlap of overall occupancy estimates. The relative rank correlation evaluated the spatial patterns in relative occupancy and provided a similarity statistic between models from −1 to 1 with a value of 1 indicating perfect positive correlation in occupancy estimates and −1 indicates perfect negative correlation.

Scenario	Relative Rank Correlation	Density Plot
A) No change	High	High
B) Decline/change in occupancy but not spatial pattern	High	Low
C) Change in spatial pattern but not occupancy	Low	High
D) Change in both occupancy and spatial pattern	Low	Low

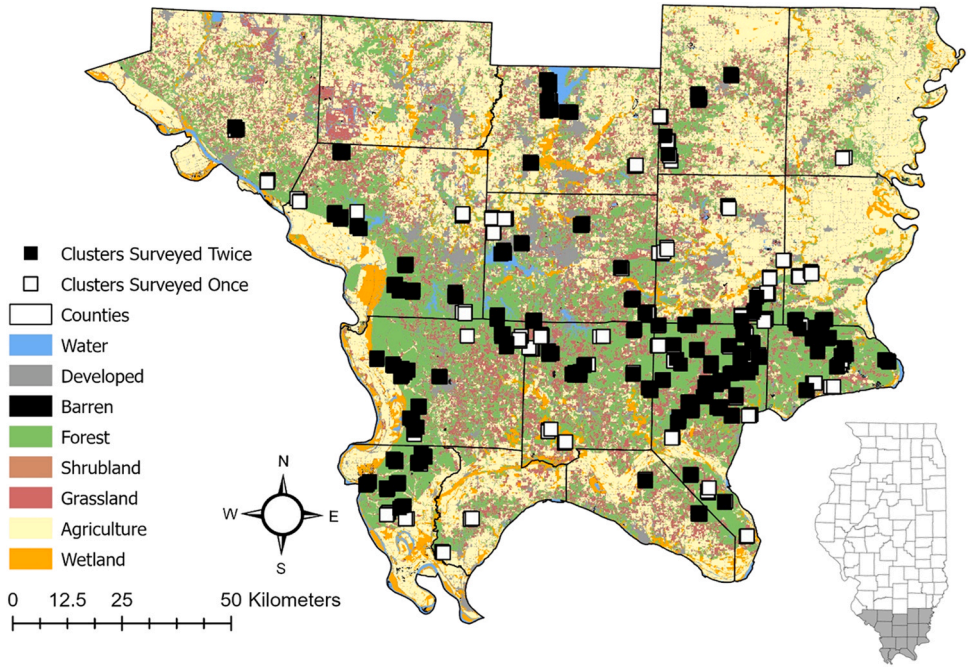

Fig. 1. Land–cover classifications, county boundaries, and survey sections (2.6–km^2) within the 16 southernmost counties of Illinois, USA, used for camera trapping, January–April 2022–2023. In 2022, 135 survey sections containing 404 individual camera traps were surveyed. In 2023, 95 survey sections containing 271 individual camera traps were resurveyed.

mays), soybeans (*Glycine max*), and winter wheat (*Triticum aestivum*; Lesmeister et al., 2015; Dewitz, 2023). Forest cover (32 %), mainly consisting of closed-canopy mixed hardwood forests, were dominated by oak-hickory species (*Acer*, *Quercus* and *Carya*; Lesmeister et al., 2015; Dewitz, 2023). Other landcover throughout the study area consisted of wetlands (6 %), open water (3 %), herbaceous and shrub/scrub lands (~1 %), with human urban and exurban development (7 %) occurring throughout (Dewitz, 2023). Stream and road densities were 1.5 km/km^2 and 1.5 km/km^2, respectively (Lesmeister et al., 2015; United States Census Bureau, 2021).

2.2. Site selection and camera trapping

January–April 2008 – 2011 field data were collected by Lesmeister et al. (2015). We deployed cameras throughout the same study extent during 3 January – 22 April 2022 and 2 January – 28 April 2023 (Fig. 1) using identical field protocols to Lesmeister et al. (2015). The study area was divided into 2.6-km^2 political sections of public and private lands (Illinois State Geological Survey, 2004). Percentage of landcover within each political section was determined using the United States Geological Survey (USGS) National Land Cover Database (USGS ,2007). Lesmeister et al. (2015) removed any political sections that contained < 11 % forest cover because their study species, bobcats (*Lynx rufus*) and gray foxes, were unlikely to occupy areas with little forest cover (Nielsen and Woolf, 2002) and the remainder of their political sections were stratified by increments of 10 % forest cover. Political sections that contained > 11 % forest cover became potential survey sections. All GIS analyses used ArcGIS Pro (Environmental Systems Research Institute [ESRI] 2023).

We selected survey sections from a candidate set of 357 2.6-km^2 survey sections created by Lesmeister et al. (2015), representing a proportional number of survey sections per increment of forest cover. We selected 150 survey sections by; 1) subsampling locations containing detections of gray foxes (n = 70 sections) during 2008–2011 (Lesmeister et al., 2015), 2) subsampling within areas with highest predicted probability of gray fox occupancy (n = 70 sections) from Lesmeister et al. (2015) gray fox spatial model, and 3) local trapper knowledge of areas occupied by gray foxes (n = 10 sections). We used OnX Maps (onXmaps Inc., Missoula, MT) to gather information on landownership and requested permission to conduct research on public and private land from the land manager or landowner within each survey section. If access was not permitted, we selected another nearby survey section that had similar land cover characteristics.

Camera traps (Browning Recon Force [20.0 megapixel] digital remote cameras; Browning, Morgan, UT) were placed afield during January–April 2022–2023. Each camera trap contained a passive infrared sensor (requiring heat and motion to be triggered) set to motion-activated mode, capturing 1 photograph each time the infrared sensor was triggered followed by a 30-second delay. We placed 3 camera traps $\geq$ 250-m apart (representing one camera cluster) in each of the 150 selected survey sections for a total of 450 individual camera traps and 150 camera clusters (Fig. 1). Camera clusters represented the 3 camera traps within each survey section. Each camera trap was secured to a nearby tree 0.5 m off the ground, faced north or south to avoid sun exposure, and baited with sardines. If game

trails were present, we placed camera traps facing towards the trail to increase detections. Each camera cluster contained 3 cameras that stayed active in the field for 21 days, providing 3 1-week survey sampling periods, and were checked every 7 days for maintenance (e.g., battery and SD card replacement) and bait replacement.

2.3. Habitat covariates

To account for imperfect detection of animals on our cameras we recorded 3 covariates that may influence detection: month of survey, average weekly temperature (°C), cumulative weekly precipitation (cm). The month of each survey was recorded at each site when the cameras were placed in the field. Temperature and precipitation data were calculated using Google Earth Engine and the European Centre for Medium-Range Weather Forecasts weather data (Gorelick et al., 2017; Muñoz Sabater, 2019). We calculated mean weekly temperature using hourly estimates of temperature to calculate the average temperature per survey site per survey week. We calculated cumulative precipitation by summing hourly estimates of precipitation per survey site per survey week. To obtain camera cluster estimates for our detection covariates, we calculated the average of each covariate from camera traps within each camera cluster.

We measured the same remotely sensed habitat covariates (Illinois State Geological Survey, 2005; United States Census Bureau, 2021; Dewitz, 2023) for both study periods (2008 – 2011 and 2022–2023). At each individual camera trap, we used data from the 2008 and 2021 USGS National Land Cover Database (Dewitz and USGS, 2021; Dewitz, 2023) to calculate landcover within a buffer (radius = 900 m) equal to 100 % of a gray fox's home range size in southern Illinois (2.75 km2; Cooper, 2008) for each respective study period. We developed 25 remotely sensed habitat covariates (Table 2) using ArcGIS Pro (Environmental Systems Research Institute [ESRI], 2023) and FragStats software (McGarigal et al., 2023). We calculated proximity indices for landcover to measure the spatial isolation of patches, accounting for both their size and distance from other patches. To assess the complexity of patch shapes, we used shape indices, which provide insights into irregularities in patch geometry. We calculated a clumpiness index for landcover as a metric to evaluate how spatially aggregated or fragmented a specific landcover type was. We also calculated the distances (m) of each independent camera trap to 3 anthropogenic features (major road, minor paved road, municipality, and human structure; (Illinois State Geological Survey, 2005, 2006; Pesaresi and Panagiotis, 2022; United States Census Bureau, 2023) using ArcGIS Pro (Environmental Systems Research Institute [ESRI] 2023). We calculated total length (m) of streams/shorelines, major roads (Interstate, U.S., and State recognized), and minor roads (County, Common Name, and Other) for each buffer size at each camera trap (United States Census

Table 2
Codes and descriptions for covariates used in detection and occupancy models of gray fox across the 16 southernmost counties of Illinois, USA, January–April 2008 – 2011 and 2022–2023. Each covariate was calculated for each camera trap using a 900 m buffer and averaged for each camera cluster.

Covariates	Description
TEMPERATURE[a]	Survey–week specific average temperature (°C)
PRECIPITATION[b]	Survey–week specific cumulative precipitation (m)
MONTH[a]	Month site was surveyed
YEAR[b]	Year site was surveyed
FORPI[b]	Forest proximity index
GRPI[b]	Grassland proximity index
FORPL[b]	Percentage forest landcover within buffer
AGPL[b]	Percentage agricultural landcover within buffer
GRPL[b]	Percentage herbaceous landcover within buffer
URPL[b]	Percentage urban landcover within buffer
URPD[b]	Number of urban patches per hectare
FORSI[b]	Forest shape index
GRSI[b]	Grassland shape index
WASI[b]	Water shape index
WESI[b]	Wetland shape index
AGCL[b]	Agricultural clumpiness index
ARCV[b]	Patch area coefficient of variation
DTRD[b]	Distance from camera trap to nearest minor road (m)
DTMJRD[b]	Distance from camera trap to nearest major road (m)
RDHA[b]	Length of minor roads per hectare within buffer (m/hectare)
STHA[b]	Human structures per hectare
MJRDHA[b]	Length of major roads per hectare within buffer (m/hectare)
STRMHA[b]	Length of streams per hectare within buffer (m/hectare)
DTSTRM[b]	Distance from camera trap to nearest linear water feature (m)
DTMU[b]	Distance to nearest municipality (m)
DTST[b]	Distance from camera trap to nearest human structure (m)
SDI[b]	Simpson's Diversity Index
PRIVATE[b]	Land ownership where camera traps were placed (public or private)
ED[b]	Total length of patch edge per hectare (m)

[a] Survey–specific covariates used in modeling detection.
[b] Remotely–sensed covariates calculated for each camera site, averaged for camera–cluster scale occupancy models.

Bureau, 2023). For camera cluster analyses, we calculated the average of each covariate from camera traps within each camera cluster. We scaled our habitat covariates, using a z-transformation, prior to modeling to ensure comparability and improve model performance. Before modeling, we ran a Pearson correlation analysis on all covariates; those with $|r| \geq 0.70$ were not included in the same model (Dormann et al., 2013).

2.4. Data analysis

2.4.1. Photo identification and covariate selection

Images were collected and identified to species. Total camera trap nights were calculated by summing the number of days that each camera trap was active for each season. Naïve occupancy probabilities (naïve occupancy = $[n_{detected}/n_{surveyed}]$; MacKenzie et al., 2002) across all camera clusters with a positive detection of a species on ≥ 1 camera trap was calculated.

2.4.2. Occupancy analysis

We used single-season single-species occupancy models (MacKenzie et al., 2002), using gray fox detected at camera clusters, to estimate detection, site occupancy, and the effects of measured covariates on gray fox occupancy throughout the study area for both 2008 – 2011 and 2022–2023, as independent sets of occupancy models. We used the statistical software R (R Core Team, 2021) and the R package 'unmarked' (Fiske and Chandler, 2011) to conduct occupancy analysis. First, we used sequential-by-sub-model strategies for modeling detection while holding the occupancy portion as a constant intercept model (Morin et al., 2020). Then, we held the most supported detection model constant when developing different sub-models for occupancy. Both sets of independent data used the same model structure for detection and occupancy models. Models were ranked using Akaike's Information Criterion corrected for small sample sizes (AICc; Burnham and Anderson, 2002). We used an information-theoretic approach to choose the most-supported detection model from each independent dataset (Burnham and Anderson, 2002; Arnold, 2010). Occupancy models were considered informative if they contributed to 90 % of the total weight in our candidate set of occupancy models (Burnham and Anderson, 2002).

2.4.3. Model development and comparison

We created 3 predictive models of gray fox occupancy, each with a 30 × 30-m resolution. Model 1 was developed using 2008 – 2011 model-averaged occupancy models and habitat covariates derived using 2008 habitat data. Model 2 used the same set of model-averaged occupancy models as Model 1 but used 2021 habitat data. This model was used as an indication of expected gray fox occupancy and distribution throughout the study extent assuming that only changes in habitat influenced occupancy between 2008 – 2011 and 2022–2023. Model 3 was developed using 2022–2023 model-averaged occupancy models and 2021 habitat data to provide information on the current status of gray fox occupancy and distribution.

We used model-averaging for each informative occupancy model that contributed to 90 % of the total weight in our candidate set. Model averaging is often used to combat model selection uncertainty, however, can also be very helpful when the primary goal is prediction (Arnold, 2010). Occupancy for each 30 m x 30 m grid cell within the study area was calculated using the model-specific beta coefficient estimates and covariate measurements for each grid cell (Lesmeister et al., 2015). Each grid cell was then multiplied by the model weight (w) for that specific model. This step was repeated for each model within the 90 % total candidate set weight and values were summed for each grid cell to indicate model averaged occupancy for gray foxes in each grid cell. We calculated an AUC score for both sets of model averaged occupancy models using within sample data to test for predictive capabilities prior to spatial model development.

To compare overall change in occupancy, we generated density plots to calculate overlap between pairwise occupancy estimates across all 3 spatial models. To evaluate spatial changes in occupancy spatial patterns, we used the R package 'ENMTools' (Warren et al., 2021) to calculate a relative rank correlation (Warren et al., 2008; Perkins-Taylor and Frey, 2020). The relative rank correlation provided a similarity metric between model estimates of occupancy ranging from −1–1 with a value of 1 indicating perfect positive correlation in occupancy estimates across space and −1 indicating perfect negative correlation and occupancy estimates across space were inversely related between models. Relative rank correlation evaluated the rank order of occupancy estimates rather than absolute or proportional values. Higher correlation values (closer to −1 or 1) indicated a consistent spatial pattern or ranking of regions with high or low occupancy estimates. A positive correlation meant that regions with high occupancy estimates in one model were ranked similarly in another model (independent of their actual occupancy probability), whereas a negative correlation meant regions with high occupancy estimates in one model were ranked oppositely in another model. Consequently, the relative rank correlation can vary due to shifts in the ranking of specific grid cells within overlapping areas of the spatial model.

3. Results

We used data from 357 camera clusters that were previously surveyed during 2008–2011 (Lesmeister et al., 2015). Gray fox were detected 546 times at 19.9 % of surveyed camera clusters across 29,988 trap nights. During 2022–2023, we surveyed 230 camera clusters across 17,146 trap nights (Fig. 1), collecting 194 gray fox photographs at 5.7 % of camera clusters surveyed.

3.1. Model 1 and 2 detection and occupancy models

Out of the 28 detection models, 4 were competitive (Appendix A). The top-ranked model indicated temperature influenced detection and was used in all subsequent occupancy models. Forty-two occupancy models were in the candidate set; 7 informative

models contained 90 % of the total weight (Appendix B). Mean gray fox modeled-averaged occupancy at camera clusters was 0.24. Covariates affecting occupancy were both anthropogenic and natural habitat features. There were mixed directional effects from both anthropogenic and natural habitat features on gray fox occupancy spatial patterns (Table 3). The AUC score for model averaged occupancy models for Models 1 was 69 % indicating moderate predictive power (Pearce and Ferrier, 2000).

3.2. Model 3 detection and occupancy models

Of the 28 detection models, 2 were competitive, with an additive model indicating temperature and previous detection of gray foxes was the top ranked model (Appendix C). Both detection covariates were used in all subsequent occupancy models. Thirty-nine occupancy models were in the candidate set; 19 informative models contained 90 % of the total weight (Appendix D). Mean gray fox modeled-averaged occupancy at camera clusters was 0.06. Gray fox spatial patterns were influenced by anthropogenic and natural habitat features with mixed directional effects. Directional effects of all covariates that were found in both 2008–2011 and 2022–2023 sets of occupancy models changed, with the exception of percentage forest cover, structures per hectare, and distance to major and minor roads which indicated consistent directional effects on gray fox occupancy between both independent datasets (Table 3). The AUC score for the 2022–2023 model averaged occupancy models was 72 % indicating moderate predictive power (Pearce and Ferrier, 2000).

3.3. Model comparisons

Model 1 indicated gray fox occupancy was 0.01–0.47, with a mean of 0.17 throughout our study extent (Fig. 2A). Greater occupancy was in patches in the western half of the study area with smaller patches of higher occupancy throughout the Shawnee National Forest (Fig. 2A). Agricultural and grassland areas outside of the Shawnee National Forest contained patches with the lowest occupancy with urban landcover contributing to higher occupancy in central portions of the study area. Model 2 indicated gray fox occupancy was 0.11–0.43, with a mean of 0.21 (Fig. 2B). Areas containing higher occupancy estimates mirrored predictions in Model 1, with slightly lower occupancy outside of the Shawnee National Forest and greater occupancy throughout the interior of the Shawnee National Forest boundary. The relative rank correlation was 0.75 indicating occupancy was ranked similarly across both models. Density plots of predicted occupancy between Model 1 and 2 indicated an overlap estimate of 0.60 (Fig. 3). Model 2 predicted occupancy was greater and more variable than Model 1.

Table 3
Model averaged estimates and 95 % confidence intervals for covariates containing 90 % of total weight in our candidate set of occupancy models for gray foxes in the 16 southernmost counties of Illinois, USA, January–April 2008 – 2011 and January–April 2022–2023. * - indicate covariates that were not included in the candidate set of occupancy models containing 90 % total weight.

Covariate[a]	2008–2011	2022–2023
AGPL	−0.235 (−0.955, −0.225)	0.123 (−0.374, 0.620)
ED	0.231 (0.105, 1.387)	−0.265 (−0.432, 0.974)
SDI	−0.325 (−1.695, −0.405)	0.288 (−1.014, 1.590)
URPL	0.116 (0.087, 0.971)	−0.439 (−1.626, 0.749)
ARCV	0.002 (−0.252, 0.290)	−0.002 (−0.591, 0.586)
FORPL	0.032 (0.146, 0.720)	0.271 (−0.432, 0.974)
RDHA	−0.006 (−0.477, 0.278)	0.086 (−0.498, 0.670)
URPD	−0.008 (−0.477, 0.179)	0.250 (−0.291, 0.792)
DTMJRD	0.024 (0.070, 0.736)	0.156 (−0.369, 0.680)
DTST	0.012 (−0.123, 0.530)	0.240 (−0.291, 0.792)
STHA	−0.012 (−0.643, 0.226)	−0.465 (−1.771, 0.841)
DTRD	−0.012 (−0.617, 0.216)	0.090 (−0.446, 0.625)
DTMU	−0.005 (−0.416, 0.268)	-
STRMHA	-	−0.590 (−1.196, 0.017)
PRIVATE	-	1.296 (0.042, 2.555)
GRPL	-	−0.038 (−0.624, 0.548)
FORPI	-	−0.401 (−1.059, 0.256)
GRSI	-	−0.290 (−0.748, 0.167)
FORSI	-	−0.048 (−0.623, 0.528)

[a] AGPL, percentage of camera–cluster buffer comprised of agriculture; ED, total length of patch edge per hectare (m/hectare); SDI, Simpson's diversity index; URPL, percentage of camera–cluster buffer comprised of urbanization; ARCV, patch area coefficient of variation; FORPL, percentage of camera–cluster buffer comprised of forests; RDHA, length of minor roads per hectare within buffer (m/hectare); URPD, number of urban patches per hectare; DTMJRD, distance from camera trap to nearest major road (m); DTST, distance from camera trap to nearest human structure (m); STHA, residential human structures per hectare; DTRD, distance from camera trap to nearest minor road (m); DTMU, distance to nearest municipality (m); STRMHA, length of streams per hectare within buffer (m/hectare); PRIVATE, land ownership where camera traps were placed (public or private); GRPL, percentage herbaceous landcover within buffer; FORPI, forest proximity index; GRSI, grassland shape index; FORSI, forest shape index.

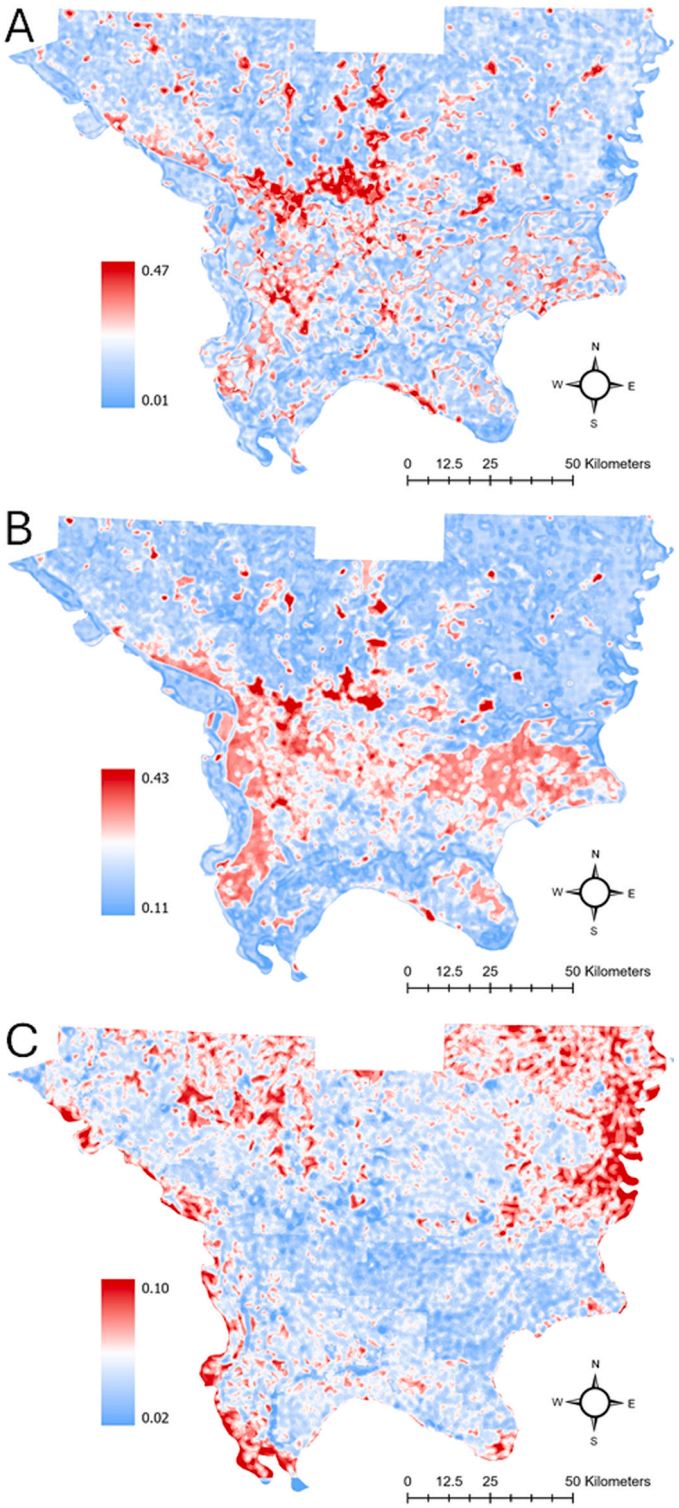

Fig. 2. Three spatial models indicating gray fox occupancy estimates and distributions throughout the southernmost 16 counties of Illinois, USA, based on 100 % home-range (camera-cluster scale) single-species single-season occupancy modeling. A) Model 1 past gray fox predictive occupancy probabilities (range $\psi = 0.01–0.47$, $\overline{\psi} = 0.17$) January–April 2008–2010. B) Model 2 future gray fox predictive occupancy probabilities (range $\psi = 0.11–0.43$, $\overline{\psi} = 0.21$) using data collected January–April 2008–2010 and contemporary remotely sensed habitat data. C) Model 3 contemporary gray fox predictive occupancy probabilities (range $\psi = 0.02–0.10$, $\overline{\psi} = 0.06$) January–April 2022–2023.

Model 3, our contemporary model, indicated gray fox occupancy ranged from 0.02–0.10, with a mean of 0.06 throughout our study extent (Fig. 2C). Areas with the highest occupancy were in the northeast and northwest sections of the study extent. The relative rank correlation between Model 1, our past model, and 3 and Model 2, our expected model, and 3 was −0.28 and −0.38, respectively, both indicating spatial patterns in gray fox occupancy had a weak negative relationship between models. Density plot overlap of occupancy was 0.04 between Models 1 and 3, and 0.00 between Models 2 and 3 which indicated important declines in occupancy estimates (Fig. 3).

4. Discussion

Our analyses demonstrated a strong decline in gray fox occupancy in southern Illinois as supported by low density plot overlap between past and contemporary models. Contrary to our expectation, relative rank correlation estimates between Model 1 and Model 3 indicated a negative correlation, highlighting a fundamental shift in gray fox ecology over that time period (; Scenario D, Table 1). Comparison of gray fox distributional patterns with Model 2 indicated that the changes in gray fox occupancy and spatial patterns are not due to changes in landscape characteristics. Additionally, density plots of Model 2 suggested mean gray fox occupancy could have increased slightly between decades based solely on landscape characteristics. This is in sharp contrast with the suggested 4-fold decrease in occupancy documented between model 1 and model 3 throughout our study area.

We hypothesized directional effects of habitat covariates on gray fox occupancy would remain consistent between our 2 datasets which we found to be rarely supported. However, Model 3 revealed a shift in the directional effects of most covariates, indicating a changing relationship between gray fox spatial patterns over time. Recent studies have demonstrated the complexity of gray fox habitat preferences, suggesting their occupancy is influenced by interspecific competition and anthropogenic landscape change, which alter their spatiotemporal dynamics (Egan et al., 2021; Morin et al., 2022). Comparing Models 1 and 2 indicated consistent occupancy estimates, with a positive relative rank correlation, thereby following our predictions. Additionally, our predictions were further validated as we found mean occupancy estimates decreased dramatically between Model 1 and Model 3, revealing a widespread decline in gray fox occupancy probabilities across > 99 % of our study area. The areas with steepest declines were dominated by urban cover or forest patches within the Shawnee National Forest. This suggested factors beyond habitat may be influencing gray fox populations, such as increased competition, predation, disease, or anthropogenic disturbance (Willingham, 2008; Lesmeister et al., 2015; Egan et al., 2021; Morin et al., 2022).

Gray fox have complex interactions with conspecifics and anthropogenic influences that may be contributing to alterations in their spatial patterns and population declines. Gray fox have resource overlap with other mesopredators; increased competition with expanding coyote (*Canis latrans*) and bobcat populations can lead to heightened stress, reduced access to resources, and direct predation (Fedriani et al., 2000; Farias et al., 2005; Levi and Wilmers, 2012; Lesmeister et al., 2015), particularly in agriculturally dominated areas that gray fox may be occupying. Exurban cover, one of the leading forms of landscape change (Vogler and Vukomanovic, 2021), exacerbates habitat fragmentation and introduces new threats to wildlife (Hansen et al., 2005; Goad et al., 2014; Lesmeister et al., 2015). This form of development not only reduces contiguous tracts of habitat essential for gray fox survival but also brings domestic dogs (Gompper, 2014; Morin et al., 2018) into closer contact with native wildlife. Domestic dogs can act as both competitors and predators, often harassing and sometimes killing gray foxes (Gehrt et al., 2009). Moreover, they can serve as vectors

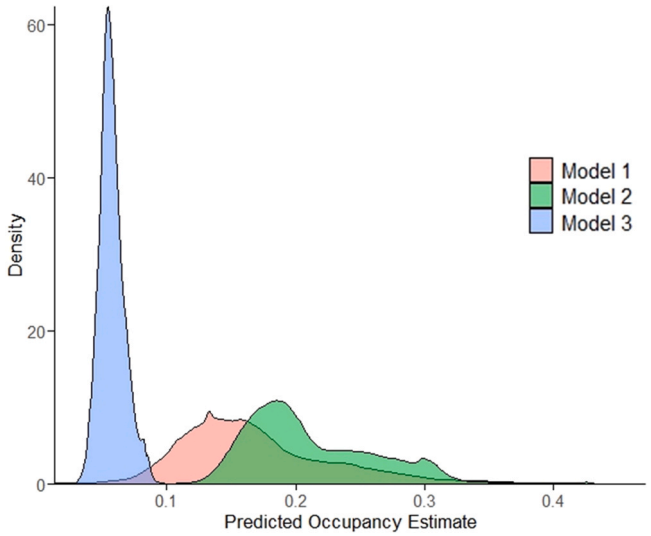

Fig. 3. Density plot of predicted gray fox occupancy estimates between Model 1, 2, and 3 based on camera trapping data collected throughout the 16 southernmost counties of Illinois, USA, January–April 2008 – 2011 and 2022–2023, based on 100 % home–range (camera–cluster scale) single–species single–season occupancy modeling. Density overlap estimates between models were: Model 1 and 2–0.60, Model 1 and 3 – 0.04, Model 2 and 3 – 0.00.

for diseases such as canine distemper (*Morbillivirus canis*), which can spread to wild populations and cause significant mortality (Pope et al., 2016).

The future of gray fox populations throughout the Midwest appears bleak and uncertain, particularly in areas where they face increasing competition from native and nonnative carnivores (Farias et al., 2005; Morin et al., 2022). Competitive pressures, where gray fox are outcompeted and even excluded by other carnivores on the landscape, suggests that without intervention, gray fox populations may continue to decline (Egan et al., 2021; Morin et al., 2022). As effective controllers of small mammal populations, gray foxes contribute to maintaining predator-prey dynamics (Chamberlain and Leopold, 2000). Additionally, gray fox population declines may decrease predation pressures of arboreal species since gray fox have the ability to climb trees, further influencing prey dynamics within both terrestrial and arboreal niches (Gunderson, 1961). As an effective seed disperser in areas of their range, decreases in the spread or germination rate of certain plant species may be influenced by gray fox population declines (Wilson, 1998). Lastly, there may be a further shift in distributions of other mesopredators with the decline or even extirpation of gray fox, potentially allowing other smaller-bodied mesopredators they directly competed with to flourish in their absence, further contributing to ecosystem instability (Willingham, 2008).

Our study emphasizes the importance of repeated collection of independent presence/absence data in wildlife research, particularly for understanding the factors driving changes in occupancy and spatial patterns (Magness et al., 2010; Perkins-Taylor and Frey, 2020). The divergence between Model 1 and 2 vs Model 3 underscores the need for periodic monitoring and adaptive management strategies, as habitat characteristics alone cannot explain the decline in gray fox occupancy. Understanding occupancy dynamics of the local carnivore guild can provide insight on population status of competing species that may be enhancing gray fox declines through increased interspecific interactions.

Ethics Statement

Not applicable: This manuscript does not include human or animal research.

Funding Statement

This research was funded by the Illinois Department of Natural Resources via Federal Aid Project W-135-R. The Cooperative Wildlife Research Laboratory, the College of Agricultural, Life and Physical Sciences, and Forestry Program at Southern Illinois University provided further support.

Declaration of Competing Interest

The authors declare that they have no known competing financial interests or personal relationships that could have appeared to influence the work reported in this paper.

Acknowledgements

Funding was provided by the Illinois Department of Natural Resources via Federal Aid Project W-135-R. The Center for Wildlife Sustainability Research; the College of Agriculture, Life and Physical Sciences; and Forestry Program at Southern Illinois University provided further support. We thank C. Dawson, D. Whipkey, J. Donovan, H. Manninen, C. Folsom, K. Place, and B. Pitman, E. La Rosa, S. Tirado, and K. Campbell for assistance with field work. We thank Dr. Jason Brown for his guidance with analytical methods. We especially thank all the private landowners, and state and federal land managers who allowed access to their properties.

Appendix A. Most supported (≤2 AIC of top model) detection models for gray foxes in the 16 southernmost counties of Illinois, USA, January–April 2008–2011

Model[a]	AICc[b]	ΔAIC	*w*[c]	*K*[d]
TEMPERATURE	634.28	0.00	0.23	3
NULL	635.88	1.60	0.10	2
TEMPERATURE + PRECIPITATION	636.00	1.72	0.10	4
TEMPERATURE + PREVIOUS DETECTION	636.11	1.83	0.09	4

[a] PRECIPITATION, cumulative precipitation for each survey week; TEMPERATURE, average temperature (°C) for each survey week; PREVIOUS DETECTION, binary variable if a gray fox was detected during the prior survey week.
[b] Akaike's Information Criterion.
[c] Model weight; probability of that model being the most supported amongst all models.
[d] Number of parameters in model.

Appendix B. Models containing 90 % of weight within the candidate set of occupancy models for gray foxes in the 16 southernmost counties of Illinois, USA, January–April 2008 – 2011

Model[a]	AICc[b]	ΔAIC	*w*[c]	*K*[d]
AGPL	623.79	0.00	0.35	4
ED + SDI	624.90	1.12	0.20	5
URPL	626.49	2.70	0.09	4
ED + ARCV + SDI	626.96	3.17	0.07	6
FORPL	627.14	3.35	0.07	4
STHA + RDHA + URPL + DTMJRD + DTST + DTRD + DTMU	627.58	3.79	0.05	10
URPL + URPD	627.73	3.95	0.05	5

[a] AGPL, percentage of camera–cluster buffer comprised of agriculture; ED, total length of patch edge per hectare (m/hectare); SDI, Simpson's diversity index; URPL, percentage of camera–cluster buffer comprised of urbanization; ARCV, patch area coefficient of variation; FORPL, percentage of camera–cluster buffer comprised of forests; STHA, residential human structures per hectare; RDHA, length of minor roads per hectare within buffer (m/hectare); URPD, number of urban patches per hectare; DTMJRD, distance from camera trap to nearest major road (m); DTST, distance from camera trap to nearest human structure (m); DTRD, distance from camera trap to nearest minor road (m); DTMU, distance to nearest municipality (m).

[b] Akaike's Information Criterion.

[c] Model weight; probability of that model being the most supported amongst all models.

[d] Number of parameters in model.

Appendix C. Most supported (≤2 AIC of top model) detection models for gray foxes in the 16 southernmost counties of Illinois, USA, January–April 2022–2023

Model[a]	AICc[b]	ΔAIC	*w*[c]	*K*[d]
TEMPERATURE + PREVIOUS DETECTION	634.28	0.00	0.23	3
PREVIOUS DETECTION	635.88	1.60	0.10	2

[a] TEMPERATURE, average temperature (°C) for each survey week; PREVIOUS DETECTION, binary variable if a gray fox was detected during the prior survey week.

[b] Akaike's Information Criterion.

[c] Model weight; probability of that model being the most supported amongst all models.

[d] Number of parameters in model.

Appendix D. Models containing 90 % of weight within the candidate set of occupancy models for gray foxes in the 16 southernmost counties of Illinois, USA, January–April 2022–2023

Model[a]	AICc[b]	ΔAIC	*w*[c]	*K*[d]
STRMHA	149.02	0.00	0.23	5
STHA	150.74	1.72	0.10	6
NULL	150.79	1.77	0.09	4
URPL	152.21	3.19	0.05	5
ED	152.43	3.40	0.04	5
DTMJRD	152.56	3.54	0.04	5
STHA	152.57	3.55	0.04	5
FORPL	152.57	3.55	0.04	5
AGPL	152.66	3.64	0.04	5
DTRD	152.78	3.75	0.03	5
RDHA	152.85	3.83	0.03	5
GRPL	152.86	3.84	0.03	5
FORPL + FORPI	153.37	4.35	0.03	6
GRSI + FORSI	153.55	4.53	0.02	6
URPL + URPD	153.57	4.55	0.02	6
STHA + DTST	153.91	4.89	0.02	6
ED + SDI	154.35	5.33	0.02	6
STHA + RDHA	154.40	5.38	0.02	6
ED + ARCV	154.53	5.51	0.01	6

[a] STRMHA, length of stream per hectare (m); STHA, residential human structures per hectare; URPL, percentage of camera–cluster buffer comprised of urbanization; ED, total length of patch edge per hectare (m/hectare); DTMJRD, distance from camera trap to nearest major road (m); FORPL, percentage of camera–cluster buffer comprised of forests; AGPL, percentage of camera–cluster buffer comprised of agriculture; DTRD, distance from camera trap to nearest minor road (m); RDHA, length of minor roads per hectare within buffer (m/hectare); GRPL, percentage herbaceous landcover within buffer; FORPI, forest proximity index; GRSI, grassland shape index; FORSI, forest shape index; URPD, number of urban patches per hectare; DTST, distance from camera trap to nearest human structure (m); SDI, Simpson's diversity index; ARCV, patch area coefficient of variation.

[b] Akaike's Information Criterion.
[c] Model weight; probability of that model being the most supported amongst all models.
[d] Number of parameters in model.

Data availability

Data will be made available on request.

References

Allen, M.L., Avrin, A.C., Farmer, M.J., Whipple, L.S., Alexander, E.P., Cervantes, A.M., Bauder, J.M., 2021. Limitations of current knowledge about the ecology of Grey Foxes hamper conservation efforts. J. Threat. Taxa 13, 19079–19092.

Amspacher, K., Jiménez, F.A., Nielsen, C., 2021. Influence of Habitat on Presence of Striped Skunks in Midwestern North America. Diversity 13, 83.

Arnold, T.W., 2010. Uninformative PArameters and Model Selection Using Akaike's Information Criterion. J. Wildl. Manag. 74, 1175–1178.

Austin, M.P., 2002. Spatial prediction of species distribution: an interface between ecological theory and statistical modelling. Ecol. Model. 157, 101–118.

Bauder, J.M., Allen, M.L., Ahlers, A.A., Benson, T.J., Miller, C.A., Stodola, K.W., 2020. Identifying and controlling for variation in canid harvest data. J. Wildl. Manag. 84, 1234–1245.

Bergstrom, B.J., 2017. Carnivore conservation: shifting the paradigm from control to coexistence. J. Mammal. 98, 1–6.

Burnham, K.P., Anderson, D.R., editors, 2002. Advanced issues and deeper insights. In: Model Selection and Multimodel Inference. Springer, New York, New York, NY, pp. 267–351.

Chamberlain, M.J., Leopold, B.D., 2000. Spatial use patterns, seasonal habitat selection, and interactions among adult gray foxes in Mississippi. J. Wildl. Manag. 64, 742–751.

Cooper, S.E., 2008. S. Surveying and Habitat Modeling for Gray Foxes in Illinois. M.S., Southern Illinois University at Carbondale, United States - Illinois.

Cooper, S.E., Nielsen, C.K., McDonald, P.T., 2012. Landscape factors affecting relative abundance of gray foxes Urocyon cinereoargenteus at large scales in Illinois, USA. Wildl. Biol. 18, 366–373.

Creel, S., Matandiko, W., Schuette, P., Rosenblatt, E., Sanguinetti, C., Banda, K., Vinks, M., Becker, M., 2018. Changes in African large carnivore diets over the past half-century reveal the loss of large prey. J. Appl. Ecol. 55, 2908–2916.

Cypher, B.L., 2003. Foxes – *Vulpes* species, *Urocyon* species, and *Alopex lagopus*. In: Feldhamer, G.A., Thompson, B.C., Chapman, J.A. (Eds.), Wild mammals of North America: biology, management, and conservation: 511–546, 2nd edn. Johns Hopkins University Press, Baltimore, Maryland, USA.

Davis, R.S., Yarnell, R.W., Gentle, L.K., Uzal, A., Mgoola, W.O., Stone, E.L., 2021. Prey availability and intraguild competition regulate the spatiotemporal dynamics of a modified large carnivore guild. Ecol. Evol. 11, 7890–7904.

Dewitz, J., 2023. National Land Cover Database (NLCD) 2021 Products: U.S. Geological Survey data release. United States Geological Survey, Sioux Falls, South Dakota, USA. https://doi.org/10.5066/P9JZ7AO3.

Dewitz, J., United States Geological Survey [USGS], 2021. National Land Cover Database (NLCD) 2019 Land Cover Conterminous United States. Multi-resolution Land Characteristics Consortium. United States Geological Survey, Sioux Falls, South Dakota, USA..

Donaldson, J.E., Hui, C., Richardson, D.M., Robertson, M.P., Webber, B.L., Wilson, J.R.U., 2014. Invasion trajectory of alien trees: the role of introduction pathway and planting history. Glob. Change Biol. 20, 1527–1537.

Dormann, C.F., Elith, J., Bacher, S., Buchmann, C., Carl, G., Carré, G., Marquéz, J.R.G., Gruber, B., Lafourcade, B., Leitão, P.J., Münkemüller, T., McClean, C., Osborne, P.E., Reineking, B., Schröder, B., Skidmore, A.K., Zurell, D., Lautenbach, S., 2013. Collinearity: a review of methods to deal with it and a simulation study evaluating their performance. Ecography 36, 27–46.

Egan, M.E., Day, C.C., Katzner, T.E., Zollner, P.A., 2021. Relative abundance of coyotes (*Canis latrans*) influences gray fox (*Urocyon cinereoargenteus*) occupancy across the eastern United States. Can. J. Zool. 99, 63–72.

Elith, J., Burgman, M.A., 2003. Habitat models for population viability analysis. In: Brigham, C.A., Schwartz, M.W. (Eds.), Population Viability in Plants: Conservation, Management, and Modeling of Rare Plants. Springer, Berlin, Heidelberg, pp. 203–235.

Elith, J., Graham, C.H., 2009. Do they? How do they? WHY do they differ? On finding reasons for differing performances of species distribution models. Ecography 32, 66–77.

Elith, J., Graham*, C.H., P. Anderson, R., Dudík, M., Ferrier, S., Guisan, A., J. Hijmans, R., Huettmann, F., R. Leathwick, J., Lehmann, A., Li, J., G. Lohmann, L., A. Loiselle, B., Manion, G., Moritz, C., Nakamura, M., Nakazawa, Y., McC. M. Overton, J., Townsend Peterson, A., J. Phillips, S., Richardson, K., Scachetti-Pereira, R., E. Schapire, R., Soberón, J., Williams, S., S. Wisz, M., E. Zimmermann, N., 2006. Novel methods improve prediction of species' distributions from occurrence data. Ecography 29, 129–151.

Environmental Systems Research Institute [ESRI], 2023. ArcGIS Pro 3.1. Redlands, CA.

Farias, V., Fuller, T.K., Wayne, R.K., Sauvajot, R.M., 2005. Survival and cause-specific mortality of gray foxes (Urocyon cinereoargenteus) in southern California. J. Zool. 266, 249–254.

Fedriani, J.M., Fuller, T.K., Sauvajot, R.M., York, E.C., 2000. Competition and intraguild predation among three sympatric carnivores. Oecologia 125, 258–270.

Fiske, I., Chandler, R., 2011. unmarked: an R package for fitting hierarchical models of wildlife occurrence and abundance. J. Stat. Softw. 43, 1–23.

Gabriel, M.W., Woods, L.W., Poppenga, R., Sweitzer, R.A., Thompson, C., Matthews, S.M., Higley, J.M., Keller, S.M., Purcell, K., Barrett, R.H., Wengert, G.M., Sacks, B. N., Clifford, D.L., 2012. Anticoagulant rodenticides on our public and community lands: spatial distribution of exposure and poisoning of a rare forest carnivore. PLoS One 7, e40163.

Gehrt, S.D., Anchor, C., White, L.A., 2009. Home range and landscape use of coyotes in a metropolitan landscape: conflict or coexistence? J. Mammal. 90, 1045–1057.

Gese, E.M., 2001. , Monitoring of terrestrial carnivore populations.

Gittleman, J.L., 1985. Carnivore body size: ecological and taxonomic correlates. Oecologia 67, 540–554.

Goad, E.H., Pejchar, L., Reed, S.E., Knight, R.L., 2014. Habitat use by mammals varies along an exurban development gradient in northern Colorado. Biol. Conserv. 176, 172–182.

Gompper, M.E. 2014. Free-Ranging Dogs and Wildlife Conservation. OUP Oxford.

Gorelick, N, Hancher, M, Dixon, M, Ilyushchenko, S, Thau, D, Moore, R, 2017. Google Earth Engine: Planetary-scale geospatial analysis for everyone. Remote Sensing of Environment 202, 18–27.

Gormley, A.M., Forsyth, D.M., Griffioen, P., Lindeman, M., Ramsey, D.S.L., Scroggie, M.P., Woodford, L., 2011. Using presence-only and presence–absence data to estimate the current and potential distributions of established invasive species. J. Appl. Ecol. 48, 25–34.

Guillera-Arroita, G., Lahoz-Monfort, J.J., Elith, J., Gordon, A., Kujala, H., Lentini, P.E., McCarthy, M.A., Tingley, R., Wintle, B.A., 2015. Is my species distribution model fit for purpose? Matching data and models to applications. Glob. Ecol. Biogeogr. 24, 276–292.

Gunderson, H.L., 1961. A Self-trapped Gray Fox. J. Mammal. 42, 270.

Hansen, A.J., Knight, R.L., Marzluff, J.M., Powell, S., Brown, K., Gude, P.H., Jones, K., 2005. Effects of exurban development on biodiversity: patterns, mechanisms, and research needs. Ecol. Appl. 15, 1893–1905.

Hedrick, B.P., Estrada, A., Sutherland, C., Barbosa, A.M., 2023. Projected northward shifts in eastern red-backed salamanders due to changing climate. Ecol. Evol. 13, e9999.
Hernandez, P.A., Graham, C.H., Master, L.L., Albert, D.L., 2006. The effect of sample size and species characteristics on performance of different species distribution modeling methods. Ecography 29, 773–785.
Illinois Department of Natural Resources [IDNR]. 2005. Illinois Comprehensive Wildlife Conservation Plan & Strategy. Springfield, Illinois.
Illinois State Geological Survey. 2004. Political townships in Illinois. Illinois State Geological Survey Geographic Information System Database. Champaign, IL, USA. (Accessed 1 October 2022). ⟨http://clearinghouse.isgs.illinois.edu/data/⟩.
Illinois State Geological Survey. 2005. Illinois digital orthophotography quarter quadrangle data. Illinois State Geological Survey Geographic Information System Database. Champaign, Illinois, USA. (Accessed 1 October 2022) ⟨http://clearinghouse.isgs.illinois.edu/data/⟩.
Illinois State Geological Survey. 2006. Municipal boundaries in Illinois: incorporated places, 2000 U.S. Census. Illinois State Geological Survey Geographic Information System Database. Champaign, IL, USA. (Accessed 1 October 2022). ⟨http://clearinghouse.isgs.illinois.edu/data/⟩.
Kwon, H.-S., Kim, B.J., Jang, G.-S., 2016. Modelling the spatial distribution of wildlife animals using presence and absence data. Contemp. Probl. Ecol. 9, 515–528.
LaRue, M.A., Nielsen, C.K., 2011. Modelling potential habitat for cougars in midwestern North America. Ecol. Model. 222, 897–900.
Lesmeister, D.B., Nielsen, C.K., Schauber, E.M., Hellgren, E.C., 2015. Spatial and temporal structure of a mesocarnivore guild in midwestern north America. Wildl. Monogr. 191, 1–61.
Levi, T., Wilmers, C.C., 2012. Wolves–coyotes–foxes: a cascade among carnivores. Ecology 93, 921–929.
MacKenzie, D.I., Nichols, J.D., Lachman, G.B., Droege, S., Andrew Royle, J., Langtimm, C.A., 2002. Estimating site occupancy rates when detection probabilities are less than one. Ecology 83, 2248–2255.
MacKenzie, D.I., Nichols, J.D., Royle, J.A., Pollock, K.H., Bailey, L., Hines, J.E., 2017. Occupancy Estimation and Modeling: Inferring Patterns and Dynamics of Species Occurrence. Elsevier.
Magness, D.R., Morton, J.M., Huettmann, F., 2010. How spatial information contributes to the conservation and management of biodiversity. In: Cushman, S.A., Huettmann, F. (Eds.), Spatial Complexity, Informatics, and Wildlife Conservation. Springer Japan, Tokyo, pp. 429–444.
Manlick, P.J., Pauli, J.N., 2020. Human disturbance increases trophic niche overlap in terrestrial carnivore communities. Proc. Natl. Acad. Sci. USA 117, 26842–26848.
Marneweck, C., Butler, A.R., Gigliotti, L.C., Harris, S.N., Jensen, A.J., Muthersbaugh, M., Newman, B.A., Saldo, E.A., Shute, K., Titus, K.L., Yu, S.W., Jachowski, D.S., 2021. Shining the spotlight on small mammalian carnivores: Global status and threats. Biol. Conserv. 255, 109005.
McGarigal K., SA Cushman, and E Ene. 2023. FRAGSTATS v4: Spatial Pattern Analysis Program for Categorical Maps. (Accessed 10 October 2024) <https://www.fragstats.org>
Meyer, N.F.V., Esser, H.J., Moreno, R., van Langevelde, F., Liefting, Y., Ros Oller, D., Vogels, C.B.F., Carver, A.D., Nielsen, C.K., Jansen, P.A., 2015. An assessment of the terrestrial mammal communities in forests of Central Panama, using camera-trap surveys. J. Nat. Conserv. 26, 28–35.
Morin, D.J., Lesmeister, D.B., Nielsen, C.K., Schauber, E.M., 2018. The truth about cats and dogs: Landscape composition and human occupation mediate the distribution and potential impact of non-native carnivores. Glob. Ecol. Conserv. 15, e00413.
Morin, D.J., Lesmeister, D.B., Nielsen, C.K., Schauber, E.M., 2022. Asymmetrical intraguild interactions with coyotes, red foxes, and domestic dogs may contribute to competitive exclusion of declining gray foxes. Ecol. Evol. 12, e9074.
Morin, D.J., Yackulic, C.B., Diffendorfer, J.E., Lesmeister, D.B., Nielsen, C.K., Reid, J., Schauber, E.M., 2020. Is your ad hoc model selection strategy affecting your multimodel inference? Ecosphere 11, e02997.
Muñoz Sabater J. 2019. ERA5-Land monthly averaged data from 1981 to present. Copernicus Climate Change Service (C3S) Climate Data Store (CDS). (Accessed 10 October 2024) <http://www.cds.climate.copernicus.eu>.
Nielsen, C.K., Woolf, A., 2002. Habitat-relative abundance relationship for Bobcats in Southern Illinois. Wildl. Soc. Bull. 30 (1973-2006), 222–230.
Pearce, J., Ferrier, S., 2000. Evaluating the predictive performance of habitat models developed using logistic regression. Ecol. Model. 133, 225–245.
Perkins-Taylor, I.E., Frey, J.K., 2020. Predicting the distribution of a rare chipmunk (Neotamias quadrivittatus oscuraensis): comparing MaxEnt and occupancy models. J. Mammal. 101, 1035–1048.
Pesaresi, M., Panagiotis, P., 2022. GHS–BUILT–C R2022A – Land Fraction as Derived from Sentinel-2 Image Composite (2018) and OSM Data. European Commission, Joint Research Centre (JRC).
Pope, J.P., Miller, D.L., Riley, M.C., Anis, E., Wilkes, R.P., 2016. Characterization of a novel Canine distemper virus causing disease in wildlife. J. Vet. Diagn. Investig. 28, 506–513.
Prugh, L.R., Stoner, C.J., Epps, C.W., Bean, W.T., Ripple, W.J., Laliberte, A.S., Brashares, J.S., 2009. The rise of the mesopredator. BioScience 59, 779–791.
R Core Team. 2021. R: A language and environment for statistical computing. Version 4.4.1. Vienna, Austria: R Foundation for Statistical Computing. <www.R–project.org.>
Rich, L.N., Davis, C.L., Farris, Z.J., Miller, D.A.W., Tucker, J.M., Hamel, S., Farhadinia, M.S., Steenweg, R., Di Bitetti, M.S., Thapa, K., Kane, M.D., Sunarto, S., Robinson, N.P., Paviolo, A., Cruz, P., Martins, Q., Gholikhani, N., Taktehrani, A., Whittington, J., Widodo, F.A., Yoccoz, N.G., Wultsch, C., Harmsen, B.J., Kelly, M. J., 2017. Assessing global patterns in mammalian carnivore occupancy and richness by integrating local camera trap surveys. Glob. Ecol. Biogeogr. 26, 918–929.
Ripple, W.J., Estes, J.A., Beschta, R.L., Wilmers, C.C., Ritchie, E.G., Hebblewhite, M., Berger, J., Elmhagen, B., Letnic, M., Nelson, M.P., Schmitz, O.J., Smith, D.W., Wallach, A.D., Wirsing, A.J., 2014. Status and ecological effects of the world's largest carnivores. Science 343, 1241484.
Street, G.M., Rodgers, A.R., Avgar, T., Vander Vennen, L.M., Fryxell, J.M., 2017. Comparing resource selection and demographic models for predicting animal density. J. Wildl. Manag. 81, 16–25.
United States Census Bureau , 2021. TIGER/Line shapefiles (machine–readable data files). Washington, D.C., USA. (Accessed 11 November 2022) ⟨http://www.census.gov/geo/maps–data/data/tiger–line.html⟩.
United States Census Bureau , 2023. County Population Totals and Components of Change: 2020-2023. Census.gov. (Accessed 11 November 2022). ⟨http://www.census.gov/data/datasets/time-series/demo/popest/2020s-counties-total.html⟩.
United States Geological Survey [USGS], 2007. National land cover database 2001. Multi-resolution Land Characteristics Consortium. (Accessed 10 November 2010)< http://www.mrlc.gov/index.php>.
Uzqueda, A., Burnett, S., Bertola, L.V., Hoskin, C.J., 2020. Quantifying range decline and remaining populations of the large marsupial carnivore of Australia's tropical rainforest. J. Mammal. 101, 1021–1034.
Vogler, J.B., Vukomanovic, J., 2021. Trends in United States human footprint revealed by new spatial metrics of urbanization and Per Capita Land Change. Sustainability 13, 12852.
Warren, D.L., Glor, R.E., Turelli, M., 2008. Environmental niche equivalency versus conservatism: quantitative approaches to niche evolution. Evolution 62, 2868–2883.
Warren, D.L., Matzke, N.J., Cardillo, M., Baumgartner, J.B., Beaumont, L.J., Turelli, M., Glor, R.E., Huron, N.A., Simões, M., Iglesias, T.L., Piquet, J.C., Dinnage, R., 2021. ENMTools 1. 0: R. Package Comp. Ecol. Biogeogr. Ecography 44, 504–511.
Williams, B.D., L.K. Campbell, C.A. Miller, and L.J. Stephens. 2020. 2019–2020 Illinois Trapper Report: Harvest, Effort, and Trapper Opinions. Technical Report INHS 2020 (29).
Willingham, A.N. 2008. Emerging Factors Associated with the Decline of A Gray Fox Population and Multi-scale Land Cover Associations of Mesopredators in the Chicago Metropolitan Area. Master's thesis. The Ohio State University. Columbus, Ohio, USA.
Wilson, J.A. 1998. Diet, Seed Dispersal Ability, and Home Range of Gray Fox (Urocyon cinereoargenteus) in Relation to Chaparral Plants of Southern California. M.A., California State University, Fullerton, United States – California.
Woolf, A., Nielsen, C.K., Weber, T., Gibbs-Kieninger, T.J., 2002. Statewide modeling of bobcat, *Lynx rufus*, habitat in Illinois, USA. Biol. Conserv. 104, 191–198.